

Recent Advances in the Description of Electromagnetic Two-Nucleon Knockout Reactions *

C. Giusti, F.D. Pacati

Dipartimento di Fisica Nucleare e Teorica, Università degli Studi di Pavia,
and Istituto Nazionale di Fisica Nucleare, Sezione di Pavia, I-27100 Pavia, Italy

M. Schwamb

Dipartimento di Fisica, Università degli Studi di Trento,
and Istituto Nazionale di Fisica Nucleare, Gruppo Collegato di Trento, I-38100 Povo (Trento),
and European Center for Theoretical Studies in Nuclear Physics and Related Areas (ECT*)
I-38100 Villazzano (Trento), Italy

Abstract

Recent advances in the description of electromagnetic two-nucleon knockout reactions are reviewed. The sensitivity to different types of correlations and to their treatment in the nuclear wave functions, the effects of final-state interactions and the role of center-of-mass effects in connection with the problem of the lack of orthogonality between initial bound states and final scattering states obtained by the use of an energy-dependent optical-model potential are discussed. Results are presented for proton-proton and proton-neutron knockout off ^{16}O also in comparison with the available data.

1 Introduction

Since a long time electromagnetic two-nucleon knockout reactions have been devised as a preferential tool to investigate two-body correlations in nuclei [1, 2]. Indeed, the probability that a real or virtual photon is absorbed by a pair of nucleons should be a direct measurement of the correlations between the two nucleons. For an exclusive reaction the transitions amplitudes contain the two-nucleon overlap function (TOF) between the ground state of the target and the final state of the residual nucleus. In the cross section the TOF gives the two-hole spectral density function, *i.e.*

$$S(\bar{\mathbf{p}}_1, \bar{\mathbf{p}}_2; \mathbf{p}_1, \mathbf{p}_2; E_m) = \langle \Psi_i | a_{\bar{\mathbf{p}}_2}^+ a_{\bar{\mathbf{p}}_1}^+ \delta(E_m - H) a_{\bar{\mathbf{p}}_1} a_{\bar{\mathbf{p}}_2} | \Psi_i \rangle, \quad (1)$$

which in its diagonal form ($\mathbf{p}_1 = \bar{\mathbf{p}}_1$ and $\mathbf{p}_2 = \bar{\mathbf{p}}_2$) gives the joint probability of removing from the target two nucleons, with momenta \mathbf{p}_1 and \mathbf{p}_2 , leaving the

*presented by C. Giusti, E-mail: giusti@pv.infn.it, phone: +39 0382987454, fax: +39 0382526938.

residual nucleus in a state with energy E_m with respect to the target ground state. In an inclusive reaction, integrating the spectral density function over the whole energy spectrum produces the two-body density matrix $\rho(\bar{\mathbf{p}}_1, \bar{\mathbf{p}}_2, \mathbf{p}_1, \mathbf{p}_2)$, that in its diagonal form and in the coordinate representation gives the pair correlation function $f(\mathbf{r}_1, \mathbf{r}_2)$, *i.e.* the conditional probability density of finding in the target a particle at \mathbf{r}_2 if another one is known to be at \mathbf{r}_1 .

The two-nucleon overlap, the two-hole spectral function and the two-body density matrix contain information on nuclear structure and correlations. The problem is that it is not easy to disentangle these quantities from the experimental cross sections and extract clear and unambiguous information on correlations. In order to achieve this goal, along with the experimental work, a reliable theoretical model is needed, where all the ingredients are well under control.

By correlations we mean what goes beyond the independent-particle model, the mean-field approximation. Of particular interest are the short-range correlations (SRC), which are produced by the short-range repulsion of the NN-interaction. SRC are of particular relevance for pp-pairs and are essential for understanding the short-range and high-momentum properties of the nuclear wave functions. Also very interesting are the tensor correlations (TC), which are due to the strong tensor component of the NN-interaction, that is of intermediate to long-range character. TC are of particular relevance for pn-pairs. Thus SRC and TC can be investigated for pp- and pn-pairs. Such an investigation would be of great interest, since the short-range repulsion and the tensor character represent the two main features of the NN-interaction. Also very important are, however, the so-called long-range correlations (LRC) at low energy, which mainly represent the interaction of nucleons at the nuclear surface and are related to the coupling between the single-particle (s.p.) dynamics and the collective excitation modes of the nucleus. SRC, TC, and LRC are intertwined in the spectral function and in the density matrix and it is not easy to disentangle a specific contribution. A reliable model for cross section calculations requires a careful and consistent treatment of these different types of correlations. Moreover, the cross section is sensitive to the reaction mechanism.

There are two competing processes contributing to two-nucleon knockout. There is the process where the electromagnetic probe hits, through a one-body (OB) current, either nucleon of a correlated pair and both nucleons are then ejected from the nucleus. Two nucleons cannot be emitted by an OB current unless they are correlated. Thus, this process is entirely due to correlations. Two nucleons, however, can also and naturally be emitted by two-body (TB) currents, due to meson exchanges and Δ -isobar excitations, even if they are not correlated. The role and relevance of these two competing processes can be different in different situations and kinematics, but if situations can be envisaged where the OB current is dominant, these situations are very well suited to investigate correlations.

It must be noted, however, that correlations affect also the process due to the TB currents. In the model [3, 4, 5, 6] the transition amplitudes contain three main ingredients: the nuclear current, the two-nucleon scattering wave function, and the TOF, which includes correlations. The two-nucleon wave functions for the initial

and final states are consistently treated in the transition amplitudes with the OB and the TB currents. Thus, correlations affect also the contribution of the TB currents and in principle it is possible to obtain information on correlations even when the TB currents are important or dominant in the cross section.

Moreover, it is not correct to say that the contribution of the OB current is entirely due to correlations in the nuclear wave functions. In the calculation of the transition amplitudes, for the three-body system consisting of the two nucleons and the residual nucleus, it is natural to work with center-of-mass (CM) coordinates, and in the CM frame a TB operator is obtained in the transition amplitude even with an OB current [7, 8]. The relevance of this CM effect depends on the particular situation that is considered and may be large or small, but, independently of that, due to this CM effects there is a contribution to two nucleons emission with an OB current also without correlations in the nuclear wave functions.

The main features of the theoretical approach are outlined in Sec. 2. Special emphasis is devoted to the description of the recent improvements performed in comparison with earlier work. Numerical results for the exclusive pp- and pn-knockout reactions off ^{16}O are presented and discussed in Sec. 3 also in comparison with the available data. Some conclusions are drawn in Sec. 4.

2 Theoretical Framework

The basic ingredients for calculations of the reaction induced by a real or virtual photon, with momentum \mathbf{q} , where two nucleons, with momenta \mathbf{p}'_1 and \mathbf{p}'_2 , are emitted from a nucleus, are the transition matrix elements of the charge-current density operator between initial and final nuclear states, *i.e.*

$$J^\mu(\mathbf{q}) = \int \langle \Psi_f | \hat{J}^\mu(\mathbf{r}) | \Psi_i \rangle e^{i\mathbf{q}\cdot\mathbf{r}} d\mathbf{r}. \quad (2)$$

Bilinear products of these integrals give the components of the hadron tensor whose suitable combinations give all the observables available from the reaction process.

The model is based on the two assumptions of an exclusive reaction, where the residual nucleus is left in a discrete eigenstate of its Hamiltonian, and of the direct knockout mechanism. As a results of these two assumptions, the matrix elements of Eq. (2) are obtained in the form [3, 4]

$$J^\mu(\mathbf{q}) = \int \psi_f^*(\mathbf{r}_1, \mathbf{r}_2) J^\mu(\mathbf{r}, \mathbf{r}_1, \mathbf{r}_2) \psi_i(\mathbf{r}_1, \mathbf{r}_2) e^{i\mathbf{q}\cdot\mathbf{r}} d\mathbf{r} d\mathbf{r}_1 d\mathbf{r}_2. \quad (3)$$

Equation (3) contains three main ingredients: the nuclear current J^μ , the two-nucleon scattering wave function ψ_f , and the TOF ψ_i . In the model ψ_i and ψ_f are consistently derived from an energy-dependent non-Hermitian Feshbach-type Hamiltonian [2, 3]. Actually, they are eigenfunctions of this Hamiltonian and of its Hermitian conjugate at different energies: for an exclusive reaction, we select a channel and then project the initial and final nuclear states in Eq. (2) onto the selected channel subspace; as a result of the projection, we obtain the optical-model

Hamiltonian describing the interaction of the two nucleons and the residual nucleus in the eigenstate that we have selected [2, 3]. Since a fully consistent calculation of ψ_f and ψ_i as eigenfunctions of the optical-model Hamiltonian would be very difficult, some approximations are used in actual calculations.

2.1 Nuclear Current

The nuclear current operator is the sum of an OB and a TB part. The OB part contains the longitudinal charge term and the convection and spin currents. The TB currents are derived from a nonrelativistic reduction of the lowest-order Feynman diagrams with one-pion exchange. Therefore we have currents corresponding to the seagull and pion-in-flight diagrams, and to the diagrams with intermediate Δ -isobar configurations [9]. All these terms contribute to pn-knockout, while the seagull and the pion-in-flight meson-exchange currents (MEC) do not contribute to pp-emission, at least in the adopted nonrelativistic limit.

The contribution of the TB currents depends on the type of reaction, on the kinematics, on the conditions of the calculations, and, of course, on the treatment of the TB currents. The explicit expressions of the currents can be found in [9, 10, 11]. Different parametrizations have been used in previous calculations, in particular for the Δ -current. A fundamental treatment of the Δ in electromagnetic breakup reactions on complex nuclei is presently unavailable and we can only rely on approximative schemes.

In our most recent calculations [7, 8, 11], the parameters of the Δ -current are fixed considering the NN-scattering in the Δ -region, where a reasonable description of scattering data is achieved with parameters similar to the ones of the full Bonn potential [12]. For pp-knockout, besides the usual π -exchange, also ρ -exchange is included and the coupling constants are

$$\frac{f_{\pi NN}^2}{4\pi} = 0.078, \quad \frac{f_{\pi N\Delta}^2}{4\pi} = 0.224, \quad \frac{f_{\rho NN}^2}{4\pi} = 7.10, \quad \frac{f_{\rho N\Delta}^2}{4\pi} = 20.45. \quad (4)$$

Moreover, hadronic form factors are included

$$F_{xNN}(q^2) = \left(\frac{\Lambda_{xNN}^2 - m_x^2}{\Lambda_{xNN}^2 + q^2} \right)^{n_{xNN}}, \quad F_{xN\Delta}(q^2) = \left(\frac{\Lambda_{xN\Delta}^2 - m_x^2}{\Lambda_{xN\Delta}^2 + q^2} \right)^{n_{xN\Delta}}, \quad (5)$$

with $n_{xNN} = n_{xN\Delta} = 1$, and the cutoffs

$$\Lambda_{\pi NN} = 1300 \text{ MeV}, \quad \Lambda_{\pi N\Delta} = 1200 \text{ MeV}, \quad \Lambda_{\rho NN} = 1400 \text{ MeV}, \quad \Lambda_{\rho N\Delta} = 1000 \text{ MeV}. \quad (6)$$

For pn-knockout, where the TB current contains many more terms, a simpler approach is adopted [8] where only π -exchange is included and the parameters for the Δ -current are

$$\begin{aligned} \frac{f_{\pi NN}^2}{4\pi} &= 0.078, & \frac{f_{\pi N\Delta}^2}{4\pi} &= 0.35, \\ n_{\pi NN} &= n_{\pi N\Delta} = 1, & \Lambda_{\pi NN} &= \Lambda_{\pi N\Delta} = 700 \text{ MeV}. \end{aligned} \quad (7)$$

These parameters are able to give, with only π -exchange, a comparable description of the NN-scattering data. With respect to the pion-in-flight and seagull MEC, contributing only to pn-knockout, a dipole cutoff is used of 3 GeV, in accordance with the Bonn-C potential [12] which is used also in the calculation of the TOF [6] and of the mutual interaction between the two outgoing nucleons [13, 14]. This choice of parameters for the TB currents is called in the following Bonn parametrization.

The hadronic form factors defined in Eq. (5) are necessary for regularizing the interaction at short distances, where the meson-exchange picture becomes meaningless. In previous calculations [5, 6, 15] the same coupling constants as in Eq. (7) were used with a simpler regularization in coordinate space, both for the MEC and the Δ -current, which in practice is similar to an unregularized prescription ($\Lambda_{\pi NN} = \Lambda_{\pi N\Delta} \rightarrow \infty$).

2.2 Final-State Interaction

In the scattering state ψ_f the two outgoing nucleons, 1 and 2, and the residual nucleus interact via the potential

$$V_f = V^{\text{OP}}(1) + V^{\text{OP}}(2) + V^{\text{NN}}(1, 2), \quad (8)$$

where $V^{\text{OP}}(i)$ denotes the interaction between the nucleon i and the residual nucleus, described in the model by a complex optical potential, and $V^{\text{NN}}(1, 2)$ denotes the mutual interaction between the two outgoing nucleons. Only the contribution of the final-state interaction (FSI) due to $V^{\text{OP}}(i)$ was included in our first calculations. In this approximation (DW) the two-nucleon scattering wave function is given by the product of two uncoupled s.p. distorted wave functions, eigenfunctions of a phenomenological optical potential fitted to nucleon-nucleus scattering data [16]. The contribution of $V^{\text{NN}}(1, 2)$ (NN-FSI) has been studied within a perturbative approach [13, 14].

The main contribution of FSI is given in general by the optical potential, which produces an overall and substantial reduction of the calculated cross sections. This effect is important and can never be neglected. NN-FSI gives in general an enhancement of the cross section that depends strongly on the kinematics, on the type of reaction, and on the final state of the residual nucleus. It is generally larger in pp- than in pn-knockout and in electro- than in photoinduced reactions [13, 14]. In many situations the difference between the results obtained in the DW approach and in the more complete approach where also NN-FSI is included (DW-NN) is small. There are, however, also situations where this difference is large. Numerical examples are presented in Sec. 3.

2.3 Two-Nucleon Overlap Function

The TOF ψ_i contains information on nuclear structure and correlations and represents the most interesting ingredient of the model. Different approaches have

been used [4, 5, 6, 9, 15, 17] to calculate ψ_i in pp- and pn-knockout from ^{16}O . ^{16}O is a suitable target for this study, due to the presence of discrete final states in the excitation-energy spectrum of the residual nucleus, both for ^{14}C and ^{14}N , states well separated in energy and that can be separated in experiments with good energy resolution. Experimental data are available for both $^{16}\text{O}(e,e'pp)$ [18, 19, 20] and $^{16}\text{O}(e,e'pn)$ [21] reactions.

In a simpler approach [4, 9] the TOF is given by the product of a coupled and antisymmetrized shell-model (SM) pair function and a Jastrow-type central and state independent correlation function taken from [22]. In this approach (SM-SRC) only SRC are included in the correlation function and the final state of the residual nucleus is a pure two-hole state in the target. For instance, the ground state of ^{14}C is a $(p_{1/2})^{-2}$ hole in ^{16}O .

In the more sophisticated approaches [5] and [6], the TOF is obtained from the the first calculations of the two-nucleon spectral function of ^{16}O , where SRC, TC and LRC are included with some approximations but consistently. In both calculations the TOF's for low-lying states of the residual nucleus are obtained partitioning the Hilbert space onto two subspaces where SRC and LRC are separately calculated. LRC and the long-range part of TC are calculated using the self-consistent Green's function formalism [23] in an appropriate harmonic-oscillator (h.o.) basis, large enough to account for the main collective features that influence the pair removal amplitudes. The effects of SRC due to the central and tensor part at high momenta are included by defect functions, which are solutions of a Bethe-Goldstone equation where the Pauli operator considers only configurations outside the model space where LRC are calculated. Different defect functions are obtained for different relative states and the Bonn C NN-potential [12] is used in the calculations. The TOF is given by a combination of components of relative and CM motion, that are different for different final states, where the coefficients are the two-nucleon removal amplitudes which include LRC, and the defect functions, which contain SRC, are intertwined in a complicated manner.

In the more recent calculation [6] some improvements have been included with respect to the previous work [5]: i) the non-locality of the Pauli operator is computed exactly, resulting in a larger number of defect functions with a more complicate state dependence; ii) the evaluation of nuclear structure effects related to the fragmentation of the s.p. strength has been improved by applying a Faddeev technique to the description of the internal propagators in the nucleon self-energy. Moreover, both pp- and pn-pairs are calculated in [6], while only the pp-case is considered in [5]. The numerical results presented in this contribution are obtained with the more recent TOF's from [6] (SF-B).

In [15] the defect functions for pn-knockout off ^{16}O are calculated within the framework of the coupled cluster (CC) method, using the so-called S_2 approximation, and employing the Argonne V14 NN-potential [24]. Also in this calculation (SF-CC) the defect functions include SRC and TC and have a complicate state dependence. LRC, however, are accounted for in the TOF in a simpler way and only knockout of nucleons from the $0p$ shell is considered.

An alternative procedure is proposed in [17, 25], where the TOF is obtained from the asymptotic behavior of the two-body density matrix (TDM). This procedure avoids the calculation of the spectral function, but depends strongly and relies on the availability of reliable calculations of the TDM. The applicability of the procedure is shown in [17], where the TOF obtained from a simple TDM, which is calculated within the Jastrow correlation method [26] (JCM) and incorporates only SRC, is able to give numerical results that under many aspects are qualitatively similar to the results produced by more sophisticated approaches. The TDM of [26] is at present the only TDM available for these calculations. It would be interesting to check the procedure with a more complete TDM.

2.4 Center-of-Mass Effects and Orthogonality

In the calculation of the transition amplitude of Eq. (3), for the three-body system consisting of the two nucleons, 1 and 2, and of the residual nucleus B , it is natural to work with CM coordinates [3, 7, 8, 27]

$$\mathbf{r}_{1B} = \mathbf{r}_1 - \mathbf{r}_B, \quad \mathbf{r}_{2B} = \mathbf{r}_2 - \mathbf{r}_B, \quad \mathbf{r}_B = \sum_{i=3}^A \mathbf{r}_i / (A - 2). \quad (9)$$

The conjugated momenta are given by

$$\begin{aligned} \mathbf{p}_{1B} &= \frac{A-1}{A} \mathbf{p}'_1 - \frac{1}{A} \mathbf{p}'_2 - \frac{1}{A} \mathbf{p}_B, \\ \mathbf{p}_{2B} &= -\frac{1}{A} \mathbf{p}'_1 + \frac{A-1}{A} \mathbf{p}'_2 - \frac{1}{A} \mathbf{p}_B, \\ \mathbf{P} &= \mathbf{p}'_1 + \mathbf{p}'_2 + \mathbf{p}_B, \end{aligned} \quad (10)$$

where $\mathbf{p}_B = \mathbf{q} - \mathbf{p}'_1 - \mathbf{p}'_2$ is the momentum of the residual nucleus in the laboratory frame.

With the help of these relations, the transition amplitude of Eq. (3) is obtained in the following form [7, 8]

$$J^\mu(\mathbf{q}) = \int \psi_f^*(\mathbf{r}_{1B}, \mathbf{r}_{2B}) V^\mu(\mathbf{r}_{1B}, \mathbf{r}_{2B}) \psi_i(\mathbf{r}_{1B}, \mathbf{r}_{2B}) d\mathbf{r}_{1B} d\mathbf{r}_{2B}, \quad (11)$$

where for the OB current $j^{(1)\mu}$

$$V^\mu(\mathbf{r}_{1B}, \mathbf{r}_{2B}) = \exp\left(i\mathbf{q} \frac{A-1}{A} \mathbf{r}_{1B}\right) \exp\left(-i\mathbf{q} \frac{1}{A} \mathbf{r}_{2B}\right) j^{(1)\mu}(\mathbf{r}_{1B}) + (1 \leftrightarrow 2). \quad (12)$$

Similar expressions are obtained for the TB currents [7, 8].

In spite of the fact that an OB operator cannot affect two particles if they are not correlated, it can be seen from Eqs. (11) and (12) that in the CM frame the transition operator becomes a TB operator even in the case of an OB nuclear current. Only in the limit $A \rightarrow \infty$, CM effects vanish and the expression in Eq. (3) becomes zero for a pure OB current when the matrix element is calculated using

orthogonalized s.p. wave functions. This means that, due to this CM effect, for finite nuclei the OB current can give a contribution to the cross section of two-particle emission even without correlations in the nuclear wave functions [7, 8].

Independently of the specific prescriptions adopted in the calculations, a conceptual problem arises in the model, where the initial and final states, ψ_i and ψ_f , which are eigenfunctions of an energy-dependent optical-model Hamiltonian, are, as such, not orthogonal. Indeed, the process involves transitions between bound and continuum states which must be orthogonal, since they are eigenfunctions of the full nuclear many-body Hamiltonian. Orthogonality is in general lost in a model when the description is restricted to a subspace where other channels are suppressed. The description of direct knockout reactions in terms of the eigenfunctions of a complex energy-dependent optical potential considers only partially the contribution of competing inelastic channels. A consequence of the lack of orthogonality between the initial and the final state is that Eq. (11) may contain a spurious contribution, since it does not vanish when the transition operator V^μ is set equal to 1. The use of an effective nuclear current operator would remove the orthogonality defect besides taking into account space truncation effects [2, 28]. In the usual approach, however, the replacement of the effective operator by the bare nuclear current operator may introduce a spurious contribution.

In our earlier work [4, 5, 6, 9, 15, 17] the spuriousity was removed subtracting from the transition amplitude the contribution of the OB current without correlations in the nuclear wave functions. This prescription, however, subtracts, together with the spuriousity, also the CM effect given by the TB operator in Eq. (12), that is present in the OB current independently of correlations in the nuclear wave function, and that is not spurious. Moreover, the definition of a nuclear wave function without correlations is clear in the simpler approach SM-SRC, where the uncorrelated SM pair function is multiplied by a correlation function, but it is less clear in a more sophisticated approach, like SF-B, where different types of correlations are intertwined in the TOF. In this case the prescription is applied subtracting the part of the TOF without the defect functions. The defect functions, however, include only SRC, while different correlations are intertwined in the remaining part of the TOF that is subtracted. Therefore, with this prescription also part of the contribution of correlations is subtracted.

A more accurate procedure to get rid of the spuriousity is adopted in [7, 8], where orthogonality between the initial and final states is enforced by means of a Gram-Schmidt orthogonalization [29]. In this approach each one of the two s.p. distorted scattering wave functions is orthogonalized to all the s.p. SM wave functions that are used to calculate the TOF, *i.e.*, for the TOF of [6], to the h.o. states of the basis used in the calculation of the spectral function, which range from the $0s$ up to the $1p-0f$ shell, or, for the simpler SM-SRC approach, to the s.p. states used to calculate the SM pair function.

The procedure to enforce orthogonality between s.p. bound and scattering states is done accordingly with the definition of the spurious contribution, that in the limit $A \rightarrow \infty$, where CM effects are neglected, the transition amplitude vanishes for a

pure OB current sandwiched between orthogonalized s.p. wave functions.

The orthogonalization procedure adopted in our recent work [7, 8] removes the spurious contribution and includes all the CM and correlation effects that were subtracted with the previous prescription and that are not spurious. The relevance of these effects depends on the type of reaction, on the kinematics, and on the treatment of the theoretical ingredients of the model [7, 8]. In many situations the differences between the results obtained with the two procedures are small. There are, however, situations where these differences are large, and they are very large in the super-parallel kinematics. This is a kinematical setting of particular interest, since the recent $^{16}\text{O}(e,e'pp)^{14}\text{C}$ [20] and $^{16}\text{O}(e,e'pn)^{14}\text{N}$ [21] experiments carried out at MAMI are both centred on the same super-parallel kinematics.

The super-parallel kinematics was originally proposed [3] since it is particularly favourable to emphasize short-range effects and has been widely investigated in our work. Recent results [6, 7, 8, 11, 13, 14] have shown that this kinematic setting is indeed very sensitive to correlations, but it is also very sensitive to all the other ingredients of the model. Such a great sensitivity makes the super-parallel kinematics very interesting although not very suitable to isolate the specific contribution of correlations from other competing contributions. The achievement of this goal requires experiments in a wider range of kinematics which mutually supplement each other. These arguments are illustrated in the next section with some numerical examples.

3 Results

In the super-parallel kinematics the two nucleons are ejected parallel and anti-parallel to \mathbf{q} and, for a fixed value of q and of the energy transfer ω , it is possible to explore, for different values of the kinetic energies of the outgoing nucleons, all possible values of the recoil-momentum p_B .

In Fig. 1 the differential cross sections of the $^{16}\text{O}(e,e'pp)^{14}\text{C}$ reaction are displayed, as a function of p_B , for transitions to different states of ^{14}C : the 0^+ ground state, the 1^+ state at 11.31 MeV, and the 2^+ state at 7.67 MeV. The calculations have been performed in the super-parallel kinematics of the MAMI experiment [20], with the SF-B overlap function and the DW approximation for FSI. Different shapes are obtained for the cross sections to the three final states. The shape of the recoil-momentum distribution is basically driven by the CM orbital angular momentum L of the knocked out pair. Different partial waves of relative and CM motion contribute to the TOF. Each transition is characterized by different components, with specific values of L . The relative weights of these components, which are given by the two-nucleon removal amplitudes included in the TOF, determine the shape of the momentum distribution [6].

The results of the orthogonalized approach and of the previous prescription to remove the spuriousity are compared in the figure. The difference depends on the final state. For the 0^+ ground state the orthogonalized approach gives a large enhancement of the cross section calculated with the OB current. The

result is shown in the right panel, where it can be seen that the enhancement is large for values of p_B up to about 300 MeV/c, and is a factor of about 5 in the maximum region. It is shown in [7] that the enhancement is mostly due to the CM effects included in the new calculations and not to the different treatment of the spuriousity or to the restoration of orthogonality between the initial and final-state wave functions. The difference between the results of the two approaches is only slightly reduced in the final cross sections, shown in the left panel, where also the Δ -current is included. The cross section is dominated by the OB current and only a minor role is played by the Δ -current. As a consequence, also the difference between the results obtained in the orthogonalized approach with the Bonn and the unregularized parametrizations, that are also shown in the figure, is small. A small reduction of the cross section is given by the Bonn parametrization.

For the 1^+ state the difference between the results of the orthogonalized approach and the previous results is practically negligible. In this case the Δ -current gives a significant enhancement of the OB cross section, which is larger with the unregularized than with the Bonn parametrization. For the 2^+ state the orthogonalized approach gives a significant enhancement of the cross section at low values of p_B and a negligible effect at higher momenta. The main contribution to the cross section is given by the OB current, the two parametrizations of the Δ -current give a negligible difference at low values of p_B and a small reduction at larger momenta is obtained with the Bonn parametrization.

The cross sections are very sensitive to correlations and to their treatment in the TOF. An example is shown in Fig. 2, for the reaction $^{16}\text{O}(e,e'pp)^{14}\text{C}$ to the 0^+ ground state in the same super-parallel kinematics as in Fig. 1. The cross sections calculated in the orthogonalized approach with three different TOF's are compared: the TOF from the spectral function (SF-B), from the simpler approach (SM-SRC), and from the asymptotic behaviour of a TDM including only Jastrow correlations (JCM). The three cross sections are very different, both in magnitude and shape, and all of them are dominated by the OB current, at least at lower values of p_B .

The effect of the mutual interaction between the two outgoing protons (NN-FSI), which has been neglected in the calculations presented till now, is of particular relevance for the $(e,e'pp)$ reaction in the super-parallel kinematics [13, 14]. An example is shown in Fig. 3, where the cross sections calculated in the DW-NN and DW approaches are compared for the reaction $^{16}\text{O}(e,e'pp)^{14}\text{C}$ to the 0^+ ground state. Calculations have been performed with the TOF from SF-B and the Bonn parametrization for the Δ -current. The comparison with the experimental data [20] is also shown in the figure.

The contribution of NN-FSI is very large, both in the orthogonalized approach and with our previous prescription, and produces a strong enhancement of the cross section that is particularly large just when the cross section calculated in the DW approach is small. The contribution of NN-FSI is very large at large values of p_B . The DW-NN cross sections calculated in the orthogonalized and in the previous approaches are very different. The difference is mainly due to the CM and correlation effects that were neglected in the previous approach. NN-FSI can be

considered an effect of correlations between the two nucleons in the final state.

The comparison with the MAMI data [20] in Fig. 3 emphasizes the important contribution of the CM and correlation effects included in the new orthogonalized calculations, the essential role played by NN-FSI, as well as the need of a careful treatment of different types of correlations, which are consistently included in the TOF from SF-B. A different choice of the theoretical ingredients in Figs. 1-3 can give huge differences. The most refined version of the model, with the best available ingredients (the DW-NN approach with enforced orthogonality between initial and final states, the TOF from SF-B, the Bonn parametrization for the TB currents) is able to give in the best agreement in comparison to data and a reasonable description of the $^{16}\text{O}(e,e'pp)$ data.

In Fig. 4 the differential cross section of the reaction $^{16}\text{O}(e,e'pn)^{14}\text{N}$ is displayed for the transition to the 1_2^+ excited state of ^{14}N at 3.95 MeV. This is the state that is mostly populated in pn-knockout [21, 30]. Results for this transition are therefore of particular interest. Calculations have been performed, with the TOF from SF-B and the DW approximation for FSI, in the same super-parallel kinematics already considered in Figs. 1-3 and realized in the $^{16}\text{O}(e,e'pn)^{14}\text{N}$ experiment at MAMI [21]. The previous results of [6] are compared in the figure with the results of the orthogonalized approach.

The CM effects included in the orthogonalized approach give a huge enhancement of the cross section calculated with the OB current. The result is shown in the right panel of Fig. 4. The enhancement is larger than one order of magnitude at low recoil momenta and is only slightly reduced at higher momenta. The difference between the cross sections of the two approaches is reduced when the TB currents are added. The result is shown in the left panel. In the previous calculations [6] the cross section is dominated by the TB currents, in particular by the Δ -current. In contrast, the OB current dominates the cross section in the orthogonalized approach and only a small enhancement is given by the TB currents. The differences obtained in the orthogonalized approach with the Bonn and the unregularized parametrizations for the TB currents are appreciable, although not very important. The Bonn parametrization reduces the cross section by at most 30-40 %. In the final cross section the difference between the results of the two approaches remains large, a bit less than one order of magnitude at low momenta, in the maximum region, and it is still sizable, although considerably reduced, at higher momenta.

The sensitivity to the treatment of correlations is shown in Fig. 5, where the cross sections of the reaction $^{16}\text{O}(e,e'pn)^{14}\text{N}$ to the 1_2^+ state calculated in the super-parallel kinematics with the TOF's from SF-B, SF-CC, and the simpler SM-SRC are compared. The calculations have been performed with the orthogonalized approach, the DW approximation for FSI, and the Bonn parametrization for the TB currents. The three TOF's give large differences, both in the shape and in the magnitude of the cross section. With the simpler SM-SRC, where only SRC are taken into account, the contribution of the OB current is negligible and is up to about three orders of magnitude lower than the one obtained with SF-B. When the TB currents are added, the SM-SRC cross section is enhanced by about one order of magnitude, the

difference between the SM-SRC and SF-B cross sections is reduced but remains very large, up to about two orders of magnitude in the maximum region and somewhat smaller at high values of p_B .

The SM-SRC cross section is dominated by the TB currents and, as such, it is practically unaffected by the use of orthogonalized s.p. bound and scattering wave functions. Incidentally, we note that for the separate contribution of the OB current the CM effects included in the orthogonalized approach give with SM-SRC a much smaller effect than with SF-B and SF-CC, whose cross sections are, in both cases, dominated by the OB current. The dominance of the OB current is due to the very large enhancement of the OB contribution produced, both with SF-B and SF-CC, by the CM effects included in the orthogonalized approach. In the previous calculations with SF-B [6] and SF-CC [15] the cross section to the 1_2^+ state was in both cases dominated by the TB Δ -current.

The much larger contribution of the OB current found with SF-B and SF-CC emphasizes the crucial role played by TC, that are very important in pn-emission and are neglected in the simpler SM-SRC calculation. In the SF-B and SF-CC overlap functions, SRC and TC are accounted for consistently in the defect functions, which are calculated in the two TOF's within different methods.

In Fig. 5 the SF-B cross section is generally larger than the SF-CC one. The SF-B result overshoots the SF-CC one up to a factor of 6 in the maximum region. The differences are strongly reduced for values of p_B greater than 100 MeV/ c . The differences between the two cross sections are due to the different treatment of SRC, TC and LRC. A more complete calculation of LRC in an extended shell-model basis is performed in SF-B [6], where the normalization of the two-nucleon overlap amplitudes is higher than in SF-CC. The difference in the shape of the cross section is due to the different mixing of configurations in the two calculations.

The results in Fig. 5 emphasize the need of a careful and consistent treatment of different correlations in the TOF. The contribution of NN-FSI, that is very large in the super-parallel kinematics for the (e,e'pp) reaction, is strongly reduced in the same kinematics for pn-knockout, and it is quite moderate for the 1_2^+ state [8].

The strong enhancement of the cross section to the 1_2^+ state at low values of p_B , that is due to the CM effects included in the orthogonalized approach, is able to resolve the discrepancies found [21] in comparison with the experimental data and give a much better agreement [31]. A careful comparison with the data will be presented in a forthcoming paper [31].

The super-parallel kinematics is particularly sensitive to all the ingredients of the model. Different results can be obtained in different situations. A suitable choice of kinematics can be helpful to disentangle specific contributions and reduce the uncertainties on the theoretical ingredients. An example of a different kinematics is shown in Fig. 6, where the cross sections of the reactions $^{16}\text{O}(\gamma,pp)^{14}\text{C}_{\text{g.s.}}$ and $^{16}\text{O}(\gamma,pn)^{14}\text{N}$ to the 1_2^+ state are displayed, for a coplanar symmetrical kinematics with an incident photon energy $E_\gamma = 400$ MeV. In symmetrical kinematics the two nucleons are ejected at equal energies and equal but opposite angles with respect to \mathbf{q} , and different values of p_B are obtained changing the scattering angles of the

two outgoing nucleons. In this kinematics the difference between the results of the orthogonalized and the previous prescription are generally small [7, 8], and also the effects of NN-FSI are very small. The cross sections are, however, very sensitive to the parametrization of the TB-currents. The results of the Bonn and the unregularized parametrizations, which are compared in the left panel of the figure, differ by about one order of magnitude. Also for this kinematics the results are very sensitive to the treatment of correlations in the TOF. The cross sections calculated with different TOF's, which are compared in the right panels, exhibit very large differences, both in magnitude and shape.

4 Conclusions

Recent improvements in the theoretical description of electromagnetic two-nucleon knockout have been reviewed: the sensitivity to the correlations included in the nuclear wave functions, the parametrization used for the TB currents, the effects of final-state interactions, and the role of center-of-mass effects in connection with the problem of the lack of orthogonality between bound and scattering states obtained by the use of an energy-dependent optical potential. Numerical examples have been presented for pp- and pn-knockout off ^{16}O also in comparison with the available data.

The most refined version of the model, with the best available ingredients, is able to give a reasonable, although not perfect, description of the experimental data. This result is an indication that the main theoretical ingredients contributing to the cross section seem reasonably under control. The cross sections are very sensitive to correlations and to their treatment. Different type of correlations, of short-range and long-range type, are important and require a careful and consistent treatment. An essential role is played by tensor correlations in pn-knockout. The complexity of the necessary model ingredients makes it difficult to extract clear and unambiguous information on correlations from one or two “ideal” kinematics. If we want to isolate the contribution of correlations, data are needed in various kinematics which mutually supplement each other. Close collaboration between theorists and experimentalists is necessary to achieve this goal.

References

- [1] K. Gottfried, Nucl. Phys. **5**, 557 (1958); Ann. of Phys. **21**, 29 (1963);
W. Czyz and K. Gottfried, Ann. of Phys. **21**, 47 (1963).
- [2] S. Boffi, C. Giusti and F.D. Pacati, Phys. Rep. **226**, 1 (1993);
S. Boffi, C. Giusti, F.D. Pacati and M. Radici, *Electromagnetic Response of Atomic Nuclei* (Clarendon Press, Oxford, 1996).

- [3] C. Giusti and F.D. Pacati, Nucl. Phys. A **535**, 573 (1991).
- [4] C. Giusti and F.D. Pacati, Nucl. Phys. A **615**, 373 (1997).
- [5] C.Giusti *et al.*, Phys. Rev. C **57**, 1691 (1998).
- [6] C. Barbieri, C. Giusti, F.D. Pacati, W.H. Dickhoff, Phys. Rev. C **70**, 014606 (2004).
- [7] C. Giusti, F.D. Pacati, M. Schwamb, S. Boffi, Eur. Phys. J. A **31**, 155 (2007).
- [8] C. Giusti, F.D. Pacati, M. Schwamb, S. Boffi, Eur. Phys. J. A **33**, 29 (2007).
- [9] C. Giusti and F.D. Pacati, Nucl. Phys. A **641**, 297 (1998).
- [10] P. Wilhelm, H. Arenhövel, C. Giusti, F.D. Pacati, Z. Phys. A **359**, 467 (1997).
- [11] C. Giusti, F. D. Pacati, M. Schwamb, S. Boffi, Eur. Phys. J. A **26**, 209 (2005).
- [12] R. Machleidt, K. Holinde, Ch. Elster, Phys. Rep. **149**, 1 (1987).
- [13] M. Schwamb, S. Boffi, C. Giusti, and F.D. Pacati, Eur. Phys. J. A **17**, 7 (2003).
- [14] M. Schwamb, S. Boffi, C. Giusti, and F.D. Pacati, Eur. Phys. J. A **20**, 233 (2004).
- [15] C. Giusti, H. Müther, F.D. Pacati and M. Stauf, Phys. Rev. C **60**, 054608 (1999).
- [16] A. Nadasen *et al.*, Phys. Rev. C **23**, 1023 (1981).
- [17] D.N. Kadrev *et al.*, Phys. Rev. C **68**, 014617 (2003).
- [18] C.J.G. Onderwater *et al.*, Phys. Rev. Lett. **78**, 4893 (1997); Phys. Rev. Lett. **81**, 2213 (1998).
- [19] R. Starink *et al.*, Phys. Lett. B **474**, 33 (2000).
- [20] M.Kahrau, Ph. D. thesis, Johannes-Gutenberg Universität Mainz, 1999;
G. Rosner, Prog. Part. Nucl. Phys. **44**, 99 (2000);
- [21] D.G. Middleton *et al.*, Eur. Phys. J. A **29**, 261 (2006).
- [22] C.C. Gearhart, Ph. D. thesis, Washington University, St. Louis (1994);
C.C. Gearhart, and W.H. Dickhoff, private communication.
- [23] C. Barbieri, W.H. Dickhoff, Prog. Part. Nucl. Phys. **52**, 337 (2004).
- [24] R.B. Wiringa, R.A. Smith, and T.L. Ainsworth, Phys. Rev. C **29**, 1207 (1984).
- [25] A.N. Antonov *et al.*, Phys. Rev. C **59**, 722 (1999).

- [26] S.S. Dimitrova, D.N. Kadrev, A.N. Antonov, and M.V. Stoitsov, Eur. Phys. J. A **7**, 335 (2000).
- [27] D.F. Jackson, T. Berggren, Nucl. Phys. **62**, 353 (1965).
- [28] S. Boffi *et al.*, Nucl. Phys. A **379**, 509 (1982).
- [29] S. Boffi, R. Cenni, C. Giusti, F. D. Pacati, Nucl. Phys. A **420**, 38 (1984).
- [30] L. Isaksson *et al.*, Phys. Rev. Lett. **83**, 3146 (1999);
K. R. Garrow *et al.*, Phys. Rev. C **64**, 064602 (2001).
- [31] D.G. Middleton *et al.*, in preparation.

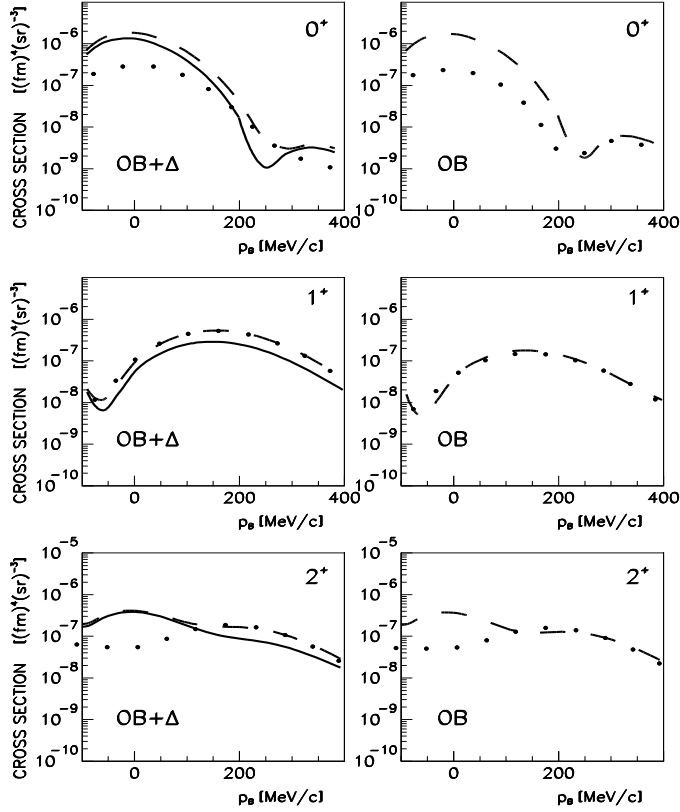


Figure 1: The differential cross section of the reaction $^{16}\text{O}(e,e'pp)^{14}\text{C}$ to the low-lying states of ^{14}C : the 0^+ ground state, the 1^+ state at 11.31 MeV, and the 2^+ state at 7.67 MeV. The super-parallel kinematics of the MAMI experiment [20] is considered, with an incident electron energy $E_0 = 855$ MeV, $\omega = 215$ MeV and $q = 316$ MeV/ c . Different values of p_B are obtained changing the kinetic energies of the two outgoing nucleons. Positive (negative) values of p_B refer to situations where p_B is parallel (anti-parallel) to q . The final results given by sum of the OB and TB Δ -current are displayed in the left panels, the separate contribution of the OB current is shown in the right panels. The TOF from [6] (SF-B) and the DW approximation for FSI are used in the calculations. The dotted lines give the results of [6], the dashed and solid lines are obtained in the orthogonalized approach with different parametrizations of the TB currents, *i.e.* the previous unregularized parametrization, as in [6], (dashed) and the Bonn parametrization (solid).

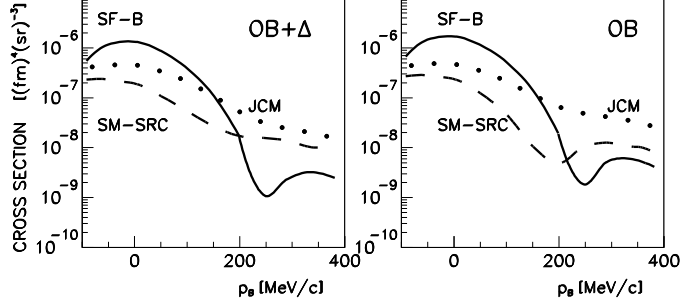


Figure 2: The differential cross section of the reaction $^{16}\text{O}(e,e'pp)^{14}\text{C}$ to the 0^+ ground state in the same super-parallel kinematics as in Fig. 1. The final results given by sum of the OB and TB Δ -current (calculated with the BONN parametrization) are displayed in the left panel, the separate contribution of the OB current is shown in the right panel. The curves are obtained in the orthogonalized approach with different TOF's: SF-B (solid), SM-SRC (dashed), JCM (dotted). The DW approximation is used for FSI.

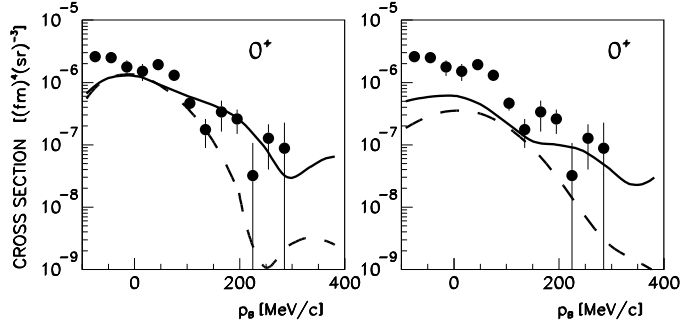


Figure 3: The differential cross section of the reaction $^{16}\text{O}(e,e'pp)^{14}\text{C}$ to the 0^+ ground state in the same super-parallel kinematics as in Fig. 1. Solid and dashed lines are obtained with the DW-NN and DW approaches for FSI. The results of the orthogonalized approach and of the previous prescription to remove the spuriousity are displayed in the left and right panels, respectively. The TOF from SF-B and the Bonn parametrization for the Δ -current are used in the calculations. Experimental data from [20].

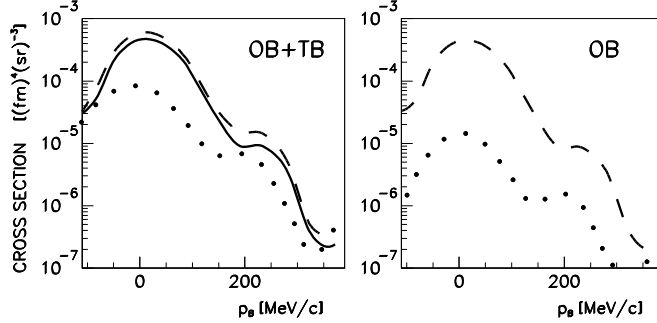


Figure 4: The differential cross section of the reaction $^{16}\text{O}(e,e'pn)^{14}\text{N}$ to the 1_2^+ state at 3.95 MeV in the same super-parallel kinematics as in Fig. 1. The proton is emitted parallel and the neutron antiparallel to the momentum transfer. The final results given by sum of the OB and TB currents are displayed in the left panel, the separate contribution of the OB current is shown in the right panel. Line convention as in Fig. 1.

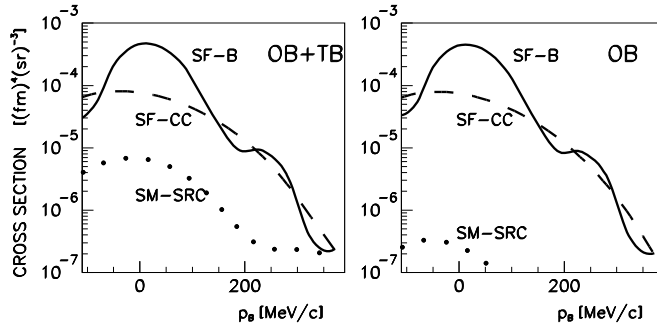


Figure 5: The differential cross section of the reaction $^{16}\text{O}(e,e'pn)^{14}\text{N}$ to the 1_2^+ state at 3.95 MeV in the same super-parallel kinematics as in Fig. 4. The curves are obtained with different TOF's: SF-B (solid), SF-CC (dashed), SM-SRC (dotted). The final results given by sum of the OB and TB currents are displayed in the left panel, the separate contribution of the OB current is shown in the right panel. Calculations are performed in the orthogonalized approach, with the DW approximation for FSI, and the Bonn parametrization for the TB currents.

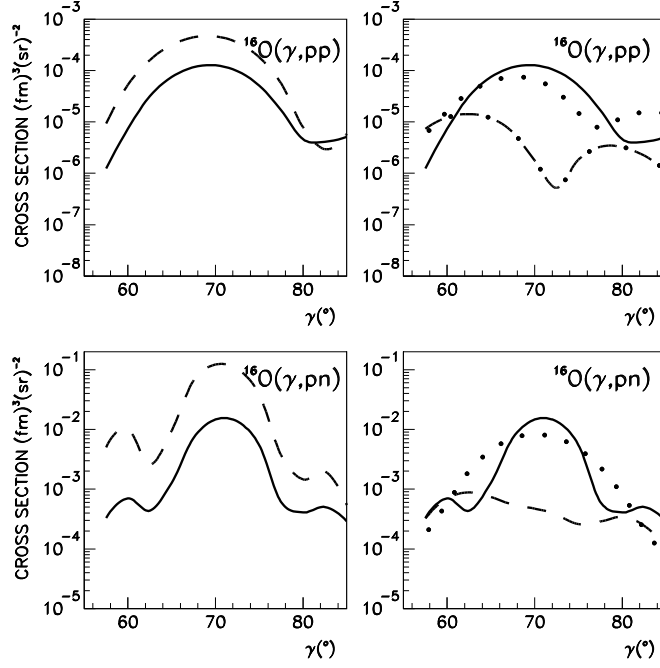


Figure 6: The differential cross section of the reactions $^{16}\text{O}(\gamma,pp)^{14}\text{C}_{\text{g.s.}}$ (top panels) and $^{16}\text{O}(\gamma,pn)^{14}\text{N}$ to the 1_2^+ state (bottom panels), in a coplanar symmetrical kinematics at $E_\gamma = 400$ MeV, as a function of the scattering angle γ of the outgoing nucleons. The results obtained with the TOF from SF-B for the Bonn (solid) and the previous unregularized parametrization (dashed) for the TB currents are compared in the left panels. The results obtained with the Bonn parametrization for different TOF's are compared in the right panels: SF-B (solid), SM-SRC (dotted), JCM (dot-dashed), SF-CC (dashed). The calculations are performed in the orthogonalized approach and with the DW approximation for FSI.